Supplemental material to this article can be found at:
http://molpharm.aspetjournals.org/content/suppl/2021/06/21/molpharm.121.000309.DC1
1521-0111/100/3/203–216$35.00
MOLECULAR PHARMACOLOGY
https://doi.org/10.1124/molpharm.121.000309
Mol Pharmacol 100:203–216, September 2021

Physiological Temperature Changes Fine-Tune β_2- Adrenergic Receptor-Induced Cytosolic cAMP Accumulation[S]

Dennis Faro, Ingrid Boekhoff, Thomas Gudermann, and Andreas Breit*

Walther-Straub-Institut für Pharmakologie und Toxikologie, Ludwig-Maximilians-Universität München, München, Germany

Received April 21, 2021; accepted June 4, 2021

ABSTRACT

Norepinephrine (NE) controls many vital body functions by activating adrenergic receptors (ARs). Average core body temperature (CBT) in mice is 37°C. Of note, CBT fluctuates between 36 and 38°C within 24 hours, but little is known about the effects of CBT changes on the pharmacodynamics of NE. Here, we used Peltier element–controlled incubators and challenged murine hypothalamic mHypoA -2/10 cells with temperature changes of ±1°C. We observed enhanced NE-induced activation of a cAMP-dependent luciferase reporter at 36 compared with 38°C. mRNA analysis and subtype specific antagonists revealed that NE activates β_2- and β_3-AR in mHypoA-2/10 cells. Agonist binding to the β_2-AR was temperature insensitive, but measurements of cytosolic cAMP accumulation revealed an increase in efficacy of 45% ± 27% for NE and of 62% ± 33% for the β_2-AR–selective agonist salmeterol at 36°C. When monitoring NE-promoted cAMP efflux, we observed an increase in the absolute efflux at 36°C. However, the ratio of exported to cytosolic accumulated cAMP is higher at 38°C. We also stimulated cells with NE at 37°C and measured cAMP degradation at 36 and 38°C afterward. We observed increased cAMP degradation at 38°C, indicating enhanced phosphodiesterase activity at higher temperatures. In line with these data, NE-induced activation of the thyreoliberin promoter was found to be enhanced at 36°C. Overall, we show that physiologic temperature changes fine-tune NE-induced cAMP signaling in hypothalamic cells via β_2-AR by modulating cAMP degradation and the ratio of intra- and extracellular cAMP.

SIGNIFICANCE STATEMENT

Increasing cytosolic cAMP levels by activation of G protein-coupled receptors (GPCR) such as the β_2-adrenergic receptor (AR) is essential for many body functions. Changes in core body temperature are fundamental and universal factors of mammalian life. This study provides the first data linking physiologically relevant temperature fluctuations to β_2-AR–induced cAMP signaling, highlighting a so far unappreciated role of body temperature as a modulator of the prototypic class A GPCR.

Introduction

Norepinephrine (NE) together with epinephrine belongs to the neurotransmitter family of catecholamines. Catecholamines bind to α_1-, α_2- and β-adrenergic receptors (ARs), which are part of the G protein-coupled receptors (GPCRs) superfamily and modulate cytosolic cAMP and Ca^{2+} levels in a variety of cells including myocytes, adipocytes, lymphocytes, keratinocytes, smooth muscle cells, and neurons (Lefkowitz et al., 1984; De Blasi, 1990; Strosberg, 1993). Consequently, signaling induced by NE via AR regulates a wide variety of vital body functions pertinent to coping with all kinds of stress and summarized as the so-called fight-or-flight response (Tank and Lee Wong, 2015).

In humans and mice, average core body temperature (CBT) is 37°C. Thus, most of our knowledge about cellular signaling induced by hormones such as NE is based on data obtained with cells stimulated at 37°C. However, depending on the species, CBT in mammals fluctuates by 1–4°C within 24 hours, with a nadir in temperature at the end of the resting state and

This work received no funding outside the Walther-Straub Institute and the Ludwig-Maximilians-Universität.
The authors declare that they have no conflicts of interest with the contents of this article.
http://dx.doi.org/10.1124/molpharm.121.000309.
[S] This article has supplemental material available at jpet.aspetjournals.org.

ABBREVIATIONS: ABCC, ATP-binding cassette subfamily C; AC, adenylyl cyclase; AR, adrenergic receptor; BAY60-6583, 2-[[6-amino-3,5-dicyano-4-[4-(cyclopropylmethoxy)phenyl]-2-pyridinyl]thio]-acetamide; BIM-X, bisindolylmaleimide X; BK, bradykinin; BMAL1, brain and muscle ARNT-like protein-1; CBT, core body temperature; CREB, cAMP response elements binding protein; CYP, cyanopindolol; DMEM, Dulbecco's modified Eagle's medium; ESI-09, α-[(2-(3-Chlorophenyl)hydrazinylidene]-5-(1,1-dimethylethyl)-β-oxo-3-isoxazolepropanenitrile; FOXO, forkhead-box-protein-O; FSK, forskolin; GPCR, G protein–coupled receptor; Gpp(NH)p, guanosine 5′-[β,γ-imido]triphosphate; HBSMC, human bronchial smooth muscle cell; ^{3}H-cAMP, adenosine 3′,5′-cyclic monophosphate [5′,8-^{3}H]; IBMX, 3-isobutyl-1-methylxantine; ICI118,551, (2*R*,3*R*)-rel-1-[(2,3-dihydro-7-methyl-1H-inden-4-yl)oxy]-3-[(1-methylethyl)amino]-2-butanol; IFN, interferon; ISO, isoproterenol; KT-5720, 2,3,9,10,11,12-hexahydro-10S-hydroxy-9-methyl-1-oxo-9R,12S-epoxy-1H-diindolo[1,2,3-fg:3′,2′,1′-kl]pyrrolo[3,4-i][1,6]benzodiazocine-10-carboxylic acid, hexylester; mHypoA-2/10, murine hypothalamic A 2/10 cells; mHypoA-2/12, murine hypothalamic A 2/12 cells; NE, norepinephrine; PDE, phosphodiesterase; PVN, paraventricular nucleus; R, active; R*, inactive; rEC-cAMP, ratio of extracellular and cytosolic cAMP; RLU, random light unit; Sal, salmeterol; signal transducer and activator of transcription; SR59230A, 1-(2-Ethylphenoxy)-3-[[(1S)-1,2,3,4-tetrahydro-1-naphthalenyl]amino]-(2S)-2-propanol hydrochloride.

a zenith during the phase of activity (Refinetti and Menaker, 1992). In humans, the amplitude of temperature change varies between 0.7 and 1.4°C, whereas in mice, changes between 1.4 and 1.8°C are described (Refinetti and Menaker, 1992).

cAMP accumulation is a popular read-out of AR signaling and the result of agonist binding to AR, G protein activation, and engagement of effector enzymes such as adenylyl cyclases (ACs) and PDE. When temperature sensitivity of AR signaling was investigated so far, temperatures used were beyond the physiological range, most probably because water baths or standard incubators had to be used, which could not ensure temperature control with an accuracy required to reliably analyze effects of small temperature changes. For example, β_2-AR–promoted contraction of guinea pig atria was stronger when 42 were compared to 27°C or 30 to 24°C (Reinhardt et al., 1978; Miyamoto et al., 2001). Walsh et al (1989) reported that β-AR–induced potassium currents in myocytes were higher at 37°C compared to 30°C (Walsh et al., 1989). AC or PDE activity in membrane fractions of hepatic cells linearly increased within a temperature range from 25 to 40°C. Interestingly, epinephrine induced a change in the thermodynamics of AC activity that led to an abrupt increase above 32°C (Keirns et al., 1973; Kreiner et al., 1973; Wada et al., 1987). In contrast, when comparing the ligand binding properties of the β_1-AR and β_2-AR in lung cells at 18 and 37°C, no differences were observed (Brodde et al., 1983). Similarly, in brown adipocytes, β-AR signaling was not affected when 37 were compared to 33°C (Ye et al., 2013). To the best of our knowledge, no data about putative effects of physiologically relevant temperature changes (±1°C) on β-AR–induced cAMP accumulation are available.

Murine and human hypothalamic neurons express relevant levels of AR, and high numbers of β-AR were found in the paraventricular nucleus (PVN) (Little et al., 1992). NE has been reported to induce mRNA levels of thyreoliberin in PVN neurons and therefore to stimulate the hypothalamic-pituitary-thyroid axes (Grimm and Reichlin, 1973). Thyreoliberin mRNA levels show circadian rhythms with peaks at the end of the resting cool phase (Covarrubias et al., 1988). Similarly, NE undergoes diurnal changes in humans and rodents, with low plasma concentrations at the end of the resting phase and increased levels during the active warm phase (Leach and Suzuki, 2020). Hence, it is stablished that NE and thyreoliberin-expressing PVN neurons interact in a circadian fashion, but it is not clear whether diurnal changes in CBT directly affect this interaction.

The adult mouse hypothalamic cell line mHypoA-2/10 expresses a wide array of hypothalamic markers (Belsham et al., 2009). We have recently reported that these cells behave similarly to thyreoliberin-positive neurons of the PVN (Breit et al., 2015, 2018). However, the responsiveness of these cells to NE has not yet been described. Herein, we first report that β_2-AR and β_3-AR subtypes are endogenously expressed in mHypoA-2/10 cells and responsible for NE-induced cAMP accumulation. Secondly, we used mHypoA-2/10 cells as an in vitro model system to analyze putative temperature effects on β-AR signaling. To appropriately challenge cells with temperature changes in the physiologic range (±1°C), we employed Peltier-element–controlled incubators (accuracy ±0.1°C). We exposed cells to 36 or 38°C and analyzed direct effects of temperature on NE binding, cytosolic cAMP accumulation, and efflux, as well as cAMP degradation and thyreoliberin promoter activity.

Materials and Methods

Materials. Dulbecco's modified Eagle's medium (DMEM) was from PanBiotech, FBS, penicillin/streptomycin, PBS, trypsin/EDTA, and Zeocin were purchased from Invitrogen (Carlsbad, CA). Turbofect was from Thermo Fisher (Heidelberg, Germany). NE, salmeterol (Sal), BK, des arginin 9 bradykinin, forskolin (FSK), SR59230A, ICI118,551, oxymetazoline, phentholamine, propranolol, Gpp(NH)p, indomethacin, and 3-isobutyl-1-methylxanthine (IBMX) were obtained from Sigma-Aldrich (Deisenhofen, Germany). ESI-09 was from Biolog (Bremen, Germany) and KT -5720 from Tocris Life Science (Lörrach, Germany). IFNγ was from Millipore. ^{125}I-cyanopindolol (CYP) and [2,8-^{3}H]-adenine was from PerkinElmer (Boston). Adenosine 3′,5′-cyclic monophosphate [5′,8-^{3}H] (^{3}H-cAMP) was from Hartmann Analytic (Braunschweig, Germany).

Cell Culture and Transfection. The adult mouse hypothalamic cell lines mHypoA-2/10 (Clu-176) and mHypoA -2/12 (CLU-177) were purchased from Cedarlane (Burlington, Canada). HaCaT cells were from the American Type Culture Collection. H1299 cells were kindly provided by Dr. Georgios Stathopoulos (CPC Helmholtz Center, Munich). All cells were cultured in DMEM supplemented with 10% FBS, 2 mM L-glutamine, penicillin (100 U/ml), and streptomycin (100 μg/ml). Human bronchial smooth muscle cells (HBSMCs) were obtained from PromoCell (C-12561) and cultured in medium provided by PromoCell. mHypoA-2/10 cell clones stably expressing the brain and muscle ARNT-like protein-1 (BMAL1)-, forkhead-box-protein-O (FOXO)-, signal transducer and activator of transcription (STAT)-, or cAMP response elements binding protein (CREB)-dependent reporter were obtained by selecting cells (400 μg/ml Zeocin) transfected with an empty pcDNA4B and the corresponding reporter plasmid. mHypoA-2/10-CREB and mHypoA-2/10-BMAL1 cells have been reported previously (Breit et al., 2018). For mHypoA-2/10-STAT cells, the pGL4.47 (luc2P/stat inducible element/Hygro) from Promega was used. For mHypoA-2/10-FOXO cells, the fas-ligand reporter element-luciferase construct was obtained from Addgene (catalog number 1789) (Brunet et al., 1999). mHypoA-2/10 cells stably expressing the entire promoter sequence of the thyreoliberin gene were generated as described above. The thyreoliberin promoter reporter plasmid was kindly provided by Dr. Clerget-Froidevaux (Kouidhi et al., 2010).

Thermostimulation. To incubate cells with high temperature accuracy (±0.1°C), two programmable, Peltier element–controlled incubators (Friocell55) from MMM group (Planegg, Germany) were used. For all experiments, cells were kept in DMEM (D5030 from Sigma-Aldrich) with 25 mM glucose, 1 mM pyruvate, 4 mM glutamine, penicillin/streptomycin, 25 mM HEPES, but without serum. pH was adjusted to 7.4 using 10 M NaOH. The following protocols were applied: 1) experiments with 37°C as a control (Figs. 1 and 4D): both incubators were first set to 37°C. After 12 hours, one incubator remained at 37°C, and the other switched within 30 minutes to 36 or 38°C, respectively. 2) Experiments without 37°C control: both incubators were first set to 37°C. After 12 hours, one incubator switched within 30 minutes to 36 and the other to 38°C, respectively. Cells were then collected at the indicated time. For the binding assay or cAMP degradation assay, incubators were set to the corresponding temperature 4 hours prior to the experiment, and all buffers needed were prewarmed for 2 hours. For the promoter reporter experiment, incubators were set to the corresponding temperature for 4 hours, the door quickly opened, cells stimulated with 10-fold ligand solutions, and incubated for another 4 hours. Temperature adjusted within 2 minutes after opening the incubator door. To measure cAMP accumulation, cells were incubated with [^{3}H]adenine for ∼20 hours and then stimulated with 10-fold IBMX or IBMX ligand solution.

Luciferase Reporter Assay. Cells were seeded on 12-well plates (∼100,000/well) and treated as described above. After stimulation, cells were lysed (25 mM Tris/HCl pH 7.4, 4 mM EGTA, 8 mM $MgCl_2$, 1 mM dithiothreitol, and 1% Triton X-100) and luciferase activity

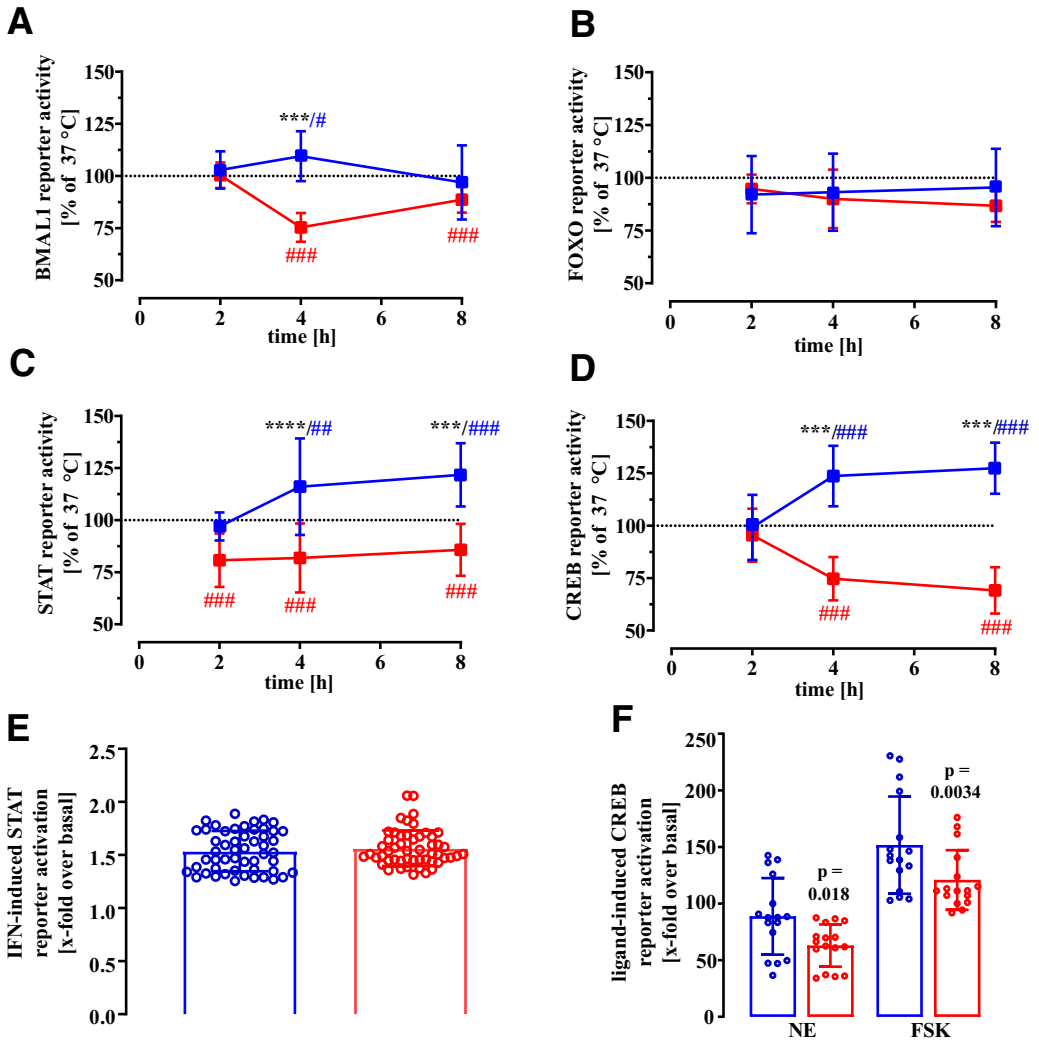

Fig. 1. Temperature sensitivity of BMAL, CREB, STAT or FOXO activity in mHypoA-2/10 cells. Basal reporter activity of BMAL1- (A), FOXO- (B), STAT- (C and E), or CREB-dependent (D and F) luciferase reporter was detected after 2, 4, or 8 hours at 36, 37, or 38°C. Data were normalized by setting data obtained at 37°C to 100%. Blue symbols present data obtained at 36°C, red symbols data at 38°C. Results are expressed as the mean ± S.D. of 6 independent experiments performed in triplicates. Asterisks indicate significant differences between 36 and 38°C using two-way ANOVA with Šidák's post hoc test. Hash signs indicate significant differences to 37°C (set to 100%) using one-sample *t* test. In (E), cells were first exposed to 36 or 38°C for 4 hours, then stimulated with IFNγ (100 nM) and in (F) with 10 μM NE or 10 μM FSK for an additional 4 hours and x-fold over basal calculated. Results are expressed as the mean ± S.D. of 4 independent experiments performed in quadruplicates. Differences between 36 and 38°C were analyzed using two-ANOVA with Šidák's post hoc test.

was measured in white bottom 96-well plates after automatically injecting luciferase substrate (Promega). Resulting total light emission was detected every second for 10 seconds postinjection in a FLUOstar Omega plate reader.

Aequorin-Based Calcium Measurements. 24 hours after transfection of ~1 × 10^6 cells with a calcium-sensing aequorin-enhanced green flourescent protein construct (pG5α, kindly provided by Dr. Chubanov, Ludwig-Maximilians-, Germany) in a 10-cm dish, cells were loaded with the aequorin substrate coelenterazine H (5 μM) in HBS buffer for 30 minutes at room temperature. After cell harvesting in HBS, ~1 × 10^5 cells per well were seeded in 96-well plates, and total luminescence was measured in a FLUOstar Omega plate reader at 37°C. Pure HBS as a control or with the corresponding ligand was automatically injected after 5 seconds. Total emission was measured at 0.5-second intervals.

Radioligand Binding Assay. At first, total membrane fractions were prepared as described previously, and aliquots stored as −80°C. For saturation binding, 20 μg of membranes were incubated with increasing concentration of ^{125}I-CYP (3.125–400 pM) in DMEM. Specific ^{125}I-CYP binding was determined by inhibition of total ^{125}I-CYP binding by 10 μM propranolol. Samples were incubated at 37°C for 1 hour and the reaction stopped by rapid filtration over Whatman GF/C glass fiber filters using a cell harvester from Brandel (Alphabiotech, Glasgow, UK). Remaining radioactivity was measured by scintillation counting using a WinSpectral1414 (PerkinElmer). Competition-binding assays were performed under the same conditions using 75 pM ^{125}I-CYP as a tracer. To uncouple GPCR from their cognate G proteins, membranes were preincubated (10 minutes) with 10 μM Gpp(NH)p.

cAMP Accumulation and Efflux. To determine agonist-induced cAMP accumulation, 100,000 cells were seeded in 12-well dishes 48 hours prior to the experiment and labeled in serum-free DMEM containing 1 μCi/ml of [^{3}H]adenine as described above. Cells were stimulated for various time periods in DMEM containing 1 mM IBMX along with NE, Sal, or FSK. The reaction was terminated by removing the medium and adding ice-cold 5% trichloroacetic acid to the cells. [^{3}H]Adenosintriphosphate and [^{3}H]cAMP were then purified by sequential chromatography (dowex-resin/aluminum oxide columns). [^{3}H]cAMP accumulation was expressed as the ratio of [cAMP/(cAMP + ATP)] x 1000. In order to determine cAMP efflux from cells, IBMX and ligand-containing medium (1 ml) were collected, reactions stopped with 1 ml of 10% trichloroacetic acid, and cAMP purified as described above. When these data are expressed as the ratio of [cAMP/(cAMP + ATP)] x 1000, cytosolic ATP levels were used.

cAMP Degradation. To determine basal cAMP degradation, 2 x 10^6 cells were seeded in 150 cm^2 dishes 24 hours prior to the experiment, serum starved overnight and harvested in 2 ml ice-cold assay buffer (50 mM HEPES 7.4, 1 mM EDTA, 0.1 mM EGTA, 10 mM $MgCl_2$, Roche cOmplete™ protease inhibitor cocktail). Cells were homogenized using a Polytron (Ultra-Turrax, T24 , IKA) 3 x 10 seconds at level 4. 100 μl total cell fraction was then added to prewarmed (36, 37, or 38°C) assay buffer (900 μl) containing ^{3}H-cAMP

(100,000 decays per minute) without IBMX or as a control with 1 mM IBMX. Samples were then incubated at the corresponding temperature for various time periods. Reactions were terminated by incubating the samples for 2 minutes at 100°C. After adding 1 ml 10% trichloroacetic acid, remaining ^{3}H-cAMP was purified as described above. As control, samples with ^{3}H-cAMP but without cell homogenates were used. These samples were used to calculate the homogenate-dependent cAMP degradation in percentage. In order to analyze effects of NE on cAMP degradation, cells were first stimulated with 10 μM NE at 37°C for 30 minutes and collected afterward.

Total mRNA Sequencing. 1×10^6 cells were seeded in six 100-cm^2 dishes. After 24 hours, cells were serum starved overnight and harvested in RNAlater (ThermoFisher). Frozen samples were sent to IMGM Laboratories (Martinsried, Germany) on dry ice and RNA sequencing was performed using the Illumina TruSeq Stranded mRNA technology and the NextSeq 500 next generation sequencing system.

Statistical Analysis. Standard sample size in this study was $n = 5$ performed in quadruplicates (or triplicates if necessary for technical reasons). If a P value of >0.05 was obtained, analysis was stopped and defined as "not statistically different." If a P value of <0.05 was determined, 3–5 additional replicates were measured to confirm statistical differences. All data are presented as the mean ± S.D. One-sample t tests were used to analyze differences to an expected value. Two-sample t tests were used to analyze experiments with two data sets. Multiple samples under one condition were analyzed by one-way ANOVA followed by Tukey's post hoc test. Multiple samples under two conditions were analyzed by two-way ANOVA followed by Tukey's or Šidák's post hoc test. P values are indicated in the figures, except for Fig. 1, where asterisks and hash signs were used for the sake of simplicity. For all analyses, GraphPad Prism 9.0 was used. Figure 11 was created using the BioRender figures software provided by BioRender.com.

Results

Effects of Temperature on BMAL1, CREB, STAT, or FOXO Reporter Activity. So far, effects of physiologically relevant temperature changes on signaling by transmembrane receptors in mHypoA-2/10 cells have not been investigated. Thus, in a first step, we analyzed basal activity of a CREB-, STAT-, and FOXO-dependent reporter. As a control, we used a BMAL1 reporter, which is temperature-sensitive in many cell types, including mHypoA-2/10 cells (Breit et al., 2018). As expected, when compared with 37°C, the activity of the BMAL1 reporter was enhanced at 36 and decreased at 38°C (Fig. 1A). The FOXO reporter showed no significant temperature sensitivity (Fig. 1B), whereas STAT- and CREB-dependent reporter activity were also enhanced at 36°C (Fig. 1, C and D). Thus, we provide the first evidence that physiologic temperature changes affect signaling pathways regulated by transmembrane receptors in hypothalamic cells and that the CREB and STAT pathways are significantly affected. Hence, in a second step, we stimulated CREB and STAT reporter–expressing cells for 4 hours either at 36 or at 38°C and then for an additional 4 hours with hormones known to activate either reporter. As shown in Fig. 1E, IFNγ activated the STAT reporter at both temperatures equally, suggesting effects of temperature on basal but not on ligand-induced STAT activation. When CREB reporter–expressing cells were stimulated with 10 μM NE, values of 63 ± 19 x-fold over basal were detected at 38°C and of 89 ± 34 at 36°C, suggesting enhanced NE effects at cooler temperature (Fig. 1F). Similarly, CREB activity induced by the direct AC activator FSK (10 μM) was also enhanced at 36°C. Thus, our data clearly indicate rather specific effects of temperature on hormone-induced CREB then on STAT activation.

mHypoA-2/10 Cells Endogenously Express the β_2-AR and β_3-AR Subtype. Members of α_1-, α_2- and β-AR subfamilies are expressed in hypothalamic neurons, but so far, no data about putative expression of AR in mHypoA-2/10 cells are available. Thus, we aimed at identifying the AR subtype(s) expressed in these cells. Total mRNAsequencing data revealed the highest expression for β_2-AR, followed by β_3-AR, and to a lesser extent by α_{1D}-AR and α_{1B}-AR (Fig. 2A). Measurements of intracellular calcium transients showed no Ca^{2+}-signals induced by NE (10 μM) or the α_2-AR agonist oxymetazoline (10 μM), suggesting no activation of Gq-coupled α-AR in hypothalamic cells. Saturation-binding experiments with the β-AR specific and β_2-AR–selective antagonist ^{125}I-cyanopindolol revealed a B_{max} of 79 ± 4 fmol/mg and a K_D-value of 28 ± 5 pM (Fig. 2C), which is characteristic of endogenously expressed β_2-AR (Chuang et al., 1986). In line with these findings, 10 μM of the β-AR–selective agonist isoproterenol (ISO) and 100 nM of the β_2-AR specific ligand Sal induced significant CREB-dependent reporter activity (Fig. 2D). NE-induced CREB activation was insensitive to the protein kinase c inhibitors BIM-X and (3-[1-[3-(dimethylamino)propyl]-5-methoxy-1H-indol-3-yl]-4-(1H-indol-3-yl)-1H-pyrrole-2,5-dione), but equally blocked by the PKA inhibitor KT-5720 or the exchange factor directly activated by cAMP inhibitor ESI-09 (Fig. 2E), providing additional hints for the involvement of β-AR rather than α-AR. To further elucidate the contribution of α-AR and β-AR subtypes, we inhibited NE-induced CREB activation with increasing concentrations of either the β_2-AR–selective antagonist ICI118,551, the β_3-AR–selective antagonist SR59 230A, or the α-AR antagonist phentolamine (Fig. 2F). Concentration-response curves with ICI118,551 or SR59230A reflected a high- and low-affinity state with almost identical fractions, indicating that NE-induced activation of the CREB reporter is mediated by β_2-AR and β_3-AR in mHypoA-2/10 cells. In line with these data, phentolamine had no inhibitory actions on NE-induced CREB activation.

Temperature Does Not Affect Binding of NE or Sal to β_2-AR in mHypoA-2/10 Cells. Ligand receptor interactions depend on the enthalpy of the reaction, which is strongly temperature-dependent (Reynolds and Holloway, 2011). Thus, we tested whether temperature would affect competition binding of NE and ^{125}I-CYP. To this end, we prepared membrane fractions of cells cultured at 37°C and performed ligand binding experiments for 1 hour at 36 or 38°C. As shown in Fig. 3A, temperature did not affect competition binding between NE and ^{125}I-CYP (IC_{50}: 1.8 ± 0.06 μM at 36°C; IC_{50}: 2.1 ± 0.08 μM at 38°C), suggesting that increased NE-induced CREB reporter activation at 36°C is not due to enhanced binding affinity of NE and β-AR. Similarly, binding of Sal to mHypoA-2/10 cells was also insensitive to temperature changes (Fig. 3B). Of note, competition-binding curves with Sal were biphasic. CYP binds to the β_2-AR with a K_D of ~10 pM and to the β_3-AR with ~500 pM (Niclauss et al., 2006). Therefore, the high-affinity site might be attributed to the β_2-AR and the low-affinity site to the β_3-AR. However, the ^{125}I-CYP concentration used (75 pM) was most probably not sufficient to detect significant amounts of the β_3-AR (calculated occupancy ≤13%). In line with this notion, the saturation-binding curve with ^{125}I-CYP shown in Fig. 2B exhibited only one phase. β_2-AR form inactive (R) and active

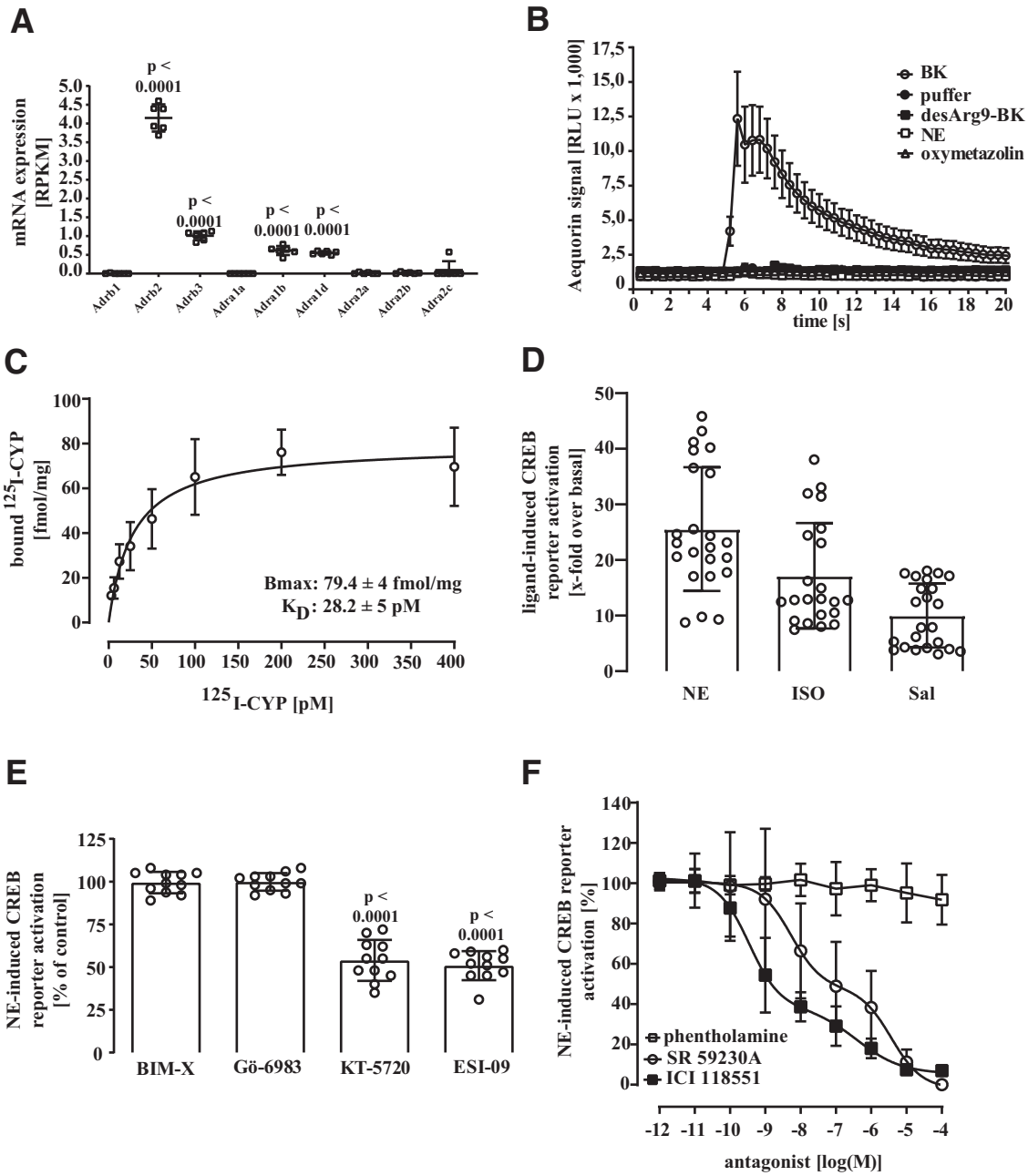

Fig. 2. mHypoA-2/10 cells express β_2-AR and β_3-AR. In (A) reads per kilobase of transcript per million reads mapped values for α_1-, α_2- and β-AR are shown as the mean ± S.D. RNAs from six distinct cell pools were used. In (B), aequorin expressing cells were stimulated with the indicated ligand by automatic injection at time point 5 second. In (C) saturation-binding experiments with total membrane fractions (20 μg) are shown. ^{125}I-CYP (3.125–400 pM) was either used alone (total binding) or together with 10 μM propranolol (unspecific binding). Receptor-bound ^{125}I-CYP was calculated by subtracting unspecific from total binding. Results of 3 independent experiments performed in triplicates are expressed as the mean ± S.D. Data were fitted using a nonlinear fit (one-site specific binding). In (D to E) data using cells stably expressing the CREB-dependent luciferase reporter are shown. In (D) serum-starved cells were stimulated or not for 4 hours at 37°C with either NE (10 μM), ISO (10 μM), or Sal (100 nM). Cells were then lysed, luciferase activity determined, and x-fold over basal calculated. Data of 5 independent experiments performed in quadruplicates are expressed as the mean ± S.D. In (E), cells were preincubated for 30 minutes with 10 μM of the PKC inhibitors BIM-X or (3-[1-[3-(dimethylamino)propyl]-5-methoxy-1H-indol-3-yl]-4-(1H-indol-3-yl)-1H-pyrrole-2,5-dione), the PKA inhibitor KT-5720, or the exchange factor directly activated by cAMP inhibitor ESI-09. In (F), serum-starved cells were stimulated for 4 hours at 37°C with either NE (10 μM) alone or together with increasing concentrations of ICI118551, SR59230A, or phentholamine. Cells were then lysed, luciferase activity determined, and data obtained with NE alone set to 100%. All other signals were calculated as percentage. Data of 6 independent experiments performed in triplicates were expressed as the mean ± S.D. and analyzed by a nonlinear fit (two-site fit logIC_{50}).

(R*) conformations. Agonists preferentially bind to and thereby stabilize R* (Samama et al., 1993). Thus, biphasic competition curves of Sal could also reflect R and R* of the β_2-AR. Formation of R* is a thermodynamic process which may be altered by physiologic temperature changes. However, no different R to R* ratios were apparent at 36 and

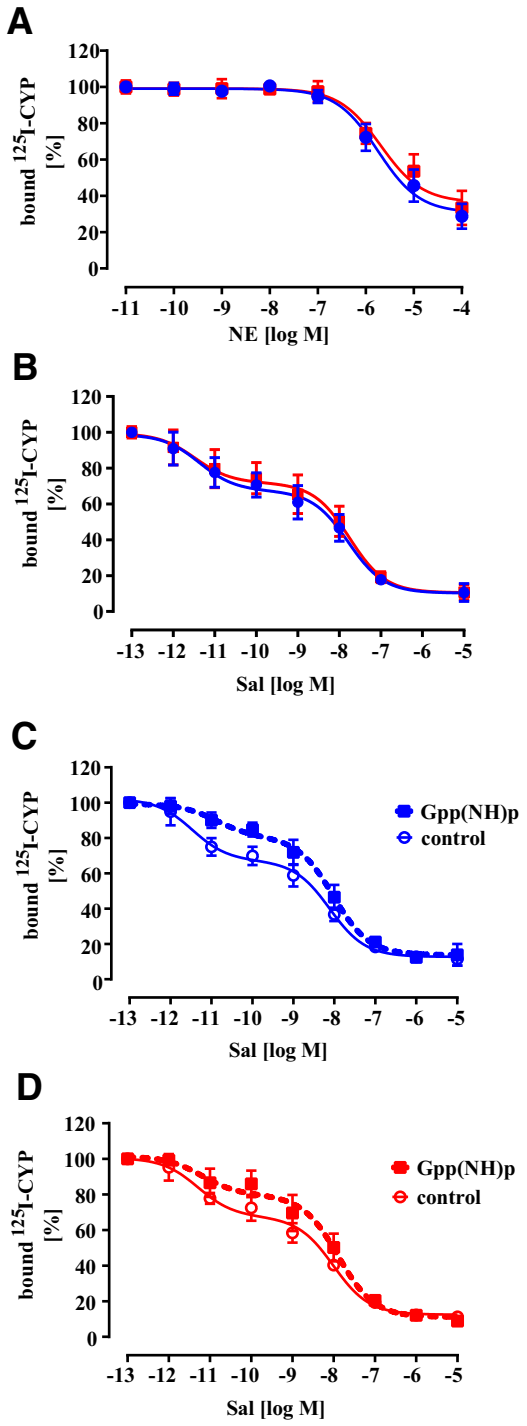

Fig. 3. Competition binding with membranes from mHypoA-2/10 cells at distinct temperatures. Competition-binding experiments with total membrane fractions (20 μg) and ^{125}I-CYP (75 pM) performed for 1 hour at 36°C (blue symbols) or at 38°C (red symbols) are shown. In (A) increasing concentrations of NE and in (B–D) of Sal were used to detect specific binding. The total ^{125}I-CYP binding in the absence of any agonist was set to 100%, and all other values calculated as percentage. In (C) and (D), membranes were preincubated or not with 10 μM of Gpp(NH)p. Data of 3 (A and B) or 4 (C and D) independent experiments performed in triplicates were expressed as the mean ± S.D and fitted using a nonlinear fit (one-site logIC_{50} in A or two-site fit logIC_{50} in B to D). Parameters of the binding curves are given in Table 1.

38°C, indicative of a lack of effects of temperature on R to R* isomerization. To substantiate this finding, we aimed at defining this relationship more precisely. R* is not only stabilized by agonists but also by the GDP-bound form of the G protein, which can be permanently transferred into the GTP-bound form by the GTP analog Gpp(NH)p (Lotti et al., 1982; Samama et al., 1993). Hence, the Gpp(NH)p-sensitive receptor population corresponds to R*. We pretreated membranes with 10 μM Gpp(NH)p and performed competition-binding experiments with ^{125}I-CYP and Sal at 36 and 38°C. In the absence of the GTP analog, we obtained almost identical biphasic competition curves at both temperatures, suggesting that physiologic temperature changes do not affect the isomerization between R and R* of the β_2-AR in mHypoA-2/10 cells (Fig. 3, C and D; Table 1). Moreover, Gpp(NH)p decreased the high-affinity state for Sal equally at both temperatures (Table 1), further strengthening the assumption that temperatures between 36 and 38°C do not affect agonist binding to the β_2-AR in mHypoA-2/10 cells.

β_2-AR–Induced Cytosolic cAMP Accumulation Is Enhanced at 36°C in mHypoA-2/10 Cells. Next, we monitored temperature sensitivity of β_2-AR–induced cytosolic cAMP accumulation in the presence of the nonselective PDE inhibitor IBMX for 1 hour. As shown in Fig. 4, A and B, NE- and Sal-promoted cytosolic cAMP accumulation was enhanced at 36°C. At 36°C, the x-fold over basal value increased from 8.3 ± 3.9 to 13.5 ± 6.5 for NE and from 10.8 ± 4.4 to 17.5 ± 10.9 for Sal compared with 38°C. When normalized to the response at 38°C, efficacy of NE-induced cAMP accumulation was enhanced by 52% ± 27% and of Sal by 62% ± 32%. Interestingly, when cAMP accumulation was induced by FSK, enhanced efficacy at 36°C was also observed (Fig. 4C). However, these effects were significantly less pronounced compared with those of NE or Sal (Fig. 4C). Our data implicate sensitivity of β_2-AR–mediated cAMP accumulation toward physiologic temperature fluctuations with increased activity at cooler temperatures. Thus, we next tested how β_2-AR–induced cAMP accumulation at 36 and 38°C would compare with 37°C. As shown in Fig. 4D, at 36°C, NE- and Sal-promoted cAMP accumulation was significantly increased compared with 37°C and decreased at 38°C, indicating an inverse correlation between temperature and β_2-AR–induced cAMP accumulation. We next performed concentration-response curves with NE to analyze effects of temperature on agonist potency (Fig. 4E). E_{max} increased from 7.5 ± 0.3 (cAMP/ATP ratio) at 38°C to 10.5 ± 0.4 at 36°C, whereas the EC_{50} values remained unchanged (3.8 ± 0.07 μM at 36°C and 4.1 ± 0.06 μM at 38°C). Thus, temperature apparently affected E_{max} but not EC_{50} values of NE in mHypoA-2/10 cells, which is in line with the observation that temperature did not affect NE binding to the β_2-AR in these cells (Fig. 3A).

Temperature Sensitivity of NE-Induced cAMP Efflux from mHypoA-2/10 Cells. To further dissect the cellular events leading to NE-induced cytosolic cAMP accumulation at lower temperatures, we determined the kinetics of this process at 37°C. As shown in Fig. 5A, NE-induced cAMP accumulation peaked at ~20 minutes, but strongly declined afterward. In fact, between 20 and 60 minutes of

TABLE 1
Competition-binding data of ^{125}I-CYP (75 pM) and Sal with 10 μM Gpp(NH)p.
Original binding curves are shown in Fig. 3, C and D

		36°C		38°C	
		pM IC_{50}	% fraction	*pM* IC_{50}	% fraction
Control	High-affinity state	3.4 ± 1.4	39 ± 2	5.6 ± 1.5	38 ± 2
	Low-affinity state	7,713 ± 657	61 ± 2	9,838 ± 1,450	62 ± 2
Ratio high-affinityto low-affinity state			0.64		0.62
Gpp(NH)p	High-affinity state	13 ± 2.4	22 ± 3	6.3 ± 2.8	24 ± 3
	Low-affinity state	9,398 ± 583	78 ± 3	12,830 ± 775	76 ± 3
Ratio high-affinityto low-affinity state			0.28		0.31

accumulation, 57% of the cAMP was lost. One explanation for this phenomenon may relate to the export of cAMP via transmembrane transporters (Godinho et al., 2015). When cAMP levels in the supernatants of the same samples shown in Fig. 5A were analyzed, a steady increase in extracellular cAMP was observed (Fig. 5B). Extracellular cAMP levels induced by NE were almost completely diminished when cAMP transporters of the ATP-binding cassette subfamily C (ABCC) were blocked by 100 μM indomethacin (Fig. 5C), indicating that the measured extracellular cAMP levels were the result of cAMP efflux (Low et al., 2020). When compiling NE-induced cAMP efflux (Fig. 5B) and cytosolic cAMP

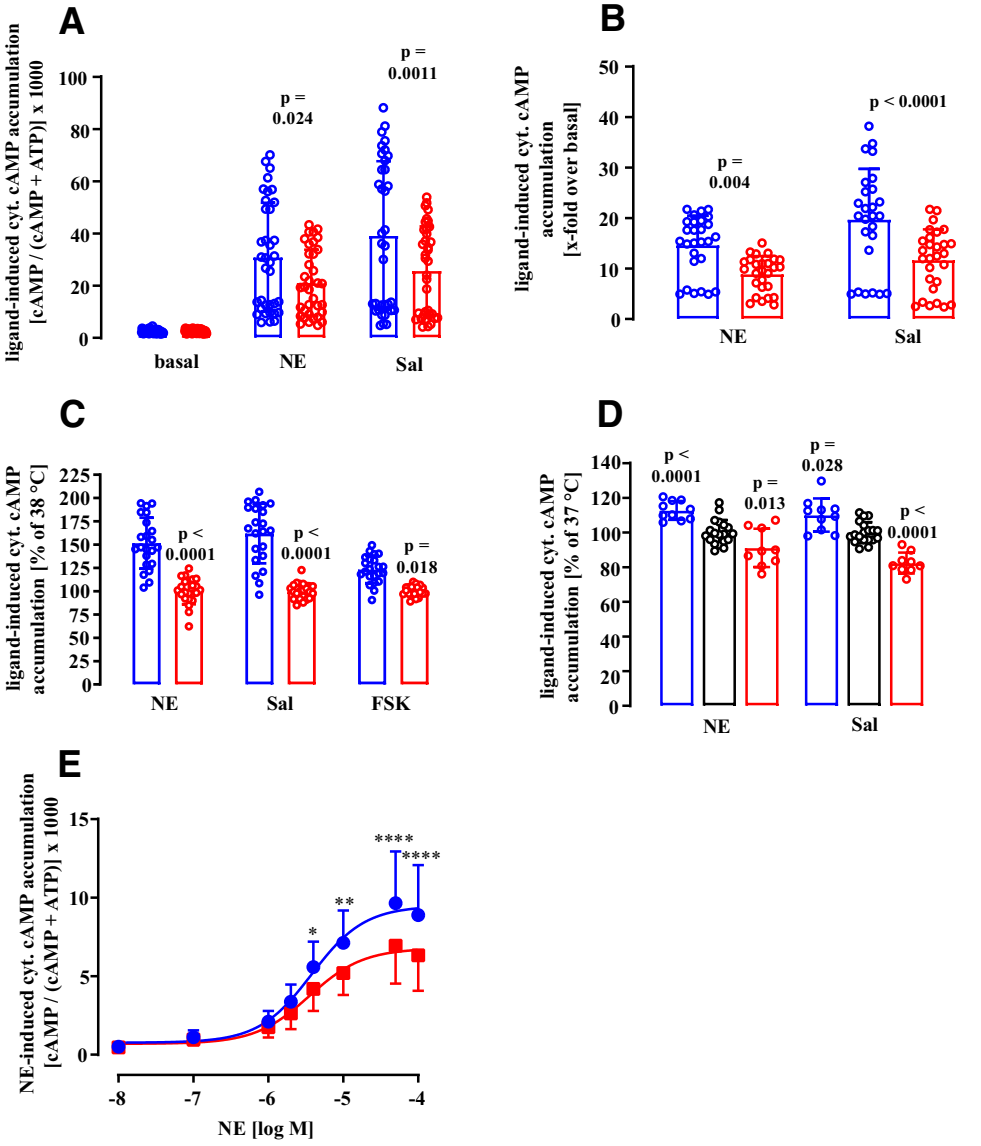

Fig. 4. NE- or Sal-induced cAMP accumulation is enhanced at 36°C. cAMP accumulation was determined for 1 hour with 1 mM IBMX alone or with NE, FSK (both 10 μM), or Sal (100 nM) in A to D. In (E) increasing concentrations of NE were used. Blue bars present data obtained at 36°C, red bars data at 38°C, and black bars at 37°C. In (A and E) data are presented as the ratio cAMP/cAMP + ATP, in (B) as x-fold over basal in (C) data obtained at 38°C and in (D) at 37°C were set to 100%. Data of 7 (A–C), 3 (D), or 4 (E) independent experiments performed in triplicates were expressed as the mean ± S.D. Data shown in (A–C) are the same. Two-way ANOVA followed by Šidák's post hoc test was used to determine statistical differences. In (E), data were fitted using a nonlinear fit ($log_{agonist}$ versus response variable slope; four parameters)

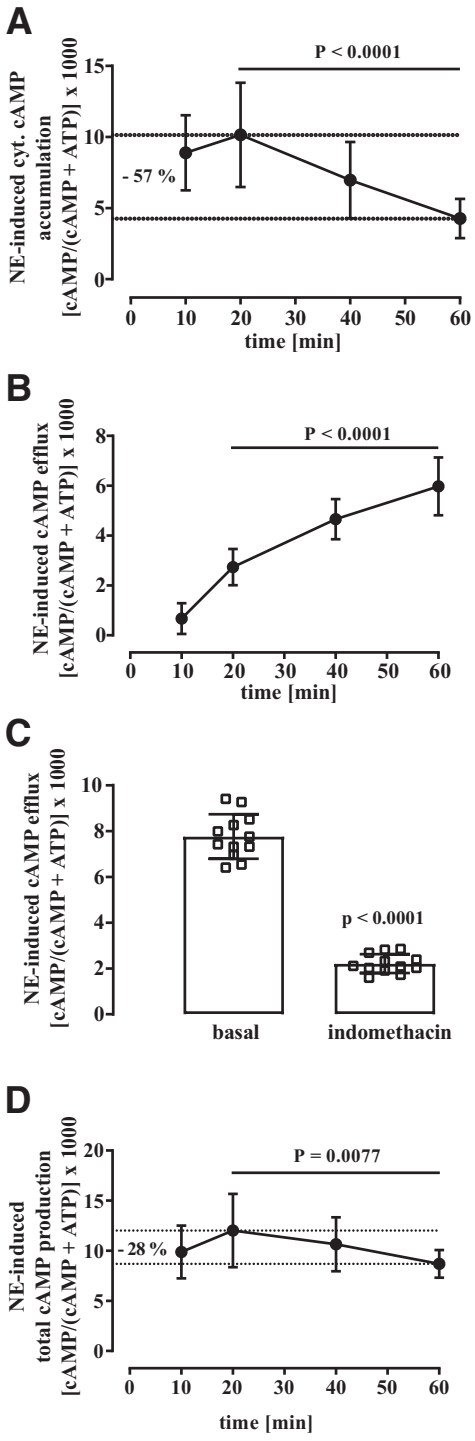

Fig. 5. NE-induced cytosolic cAMP accumulation and efflux. In (A), cytosolic cAMP accumulation for 10, 20, 40, or 60 minutes with 1 mM IBMX alone or with 10 μM NE was detected at 37°C. In (B), cAMP levels in the supernatants of the same samples are shown. In (C), cAMP levels in the supernatants of cells stimulated with 1 mM IBMX and 10 μM NE are shown in the presence or not of 100 μM indomethacin. In (D), data from (A) and (B) were compiled. Data of 4 independent experiments performed in triplicates were expressed as the mean ± S.D. One-way ANOVA followed by Tukey's post hoc test was used in (A, B, and D) and unpaired *t* test in (C) to determine statistical differences.

accumulation (Fig. 5A), we obtained total cAMP production (Fig. 5D), which now showed a decrease between 20 and 60 minutes of 28%. Thus, around half of the amount of the cAMP, which is lost from the cytosol between 20 and 60 minute of NE stimulation, is found in the supernatant.

Temperature effects on the cAMP efflux may account for enhanced cytosolic cAMP accumulation at 36°C. Therefore, we monitored cytosolic cAMP accumulation and efflux after 20 and 60 minutes of NE stimulation at 36 and 38°C. As expected, we found enhanced cAMP levels in the cytosol at 36°C after 20 and 60 minutes (Fig. 6A). Interestingly, NE-induced cAMP efflux was similar after 20 minutes, but increased after 60 minutes at 36 compared with 38°C (Fig. 6B). Assuming that cAMP efflux depends on the cytosolic cAMP concentration and is temperature-independent, the ratio of cAMP efflux and cytosolic cAMP accumulation (rEC-cAMP) is constant. However, we observed a significantly higher rEC-cAMP at 38 (1.52 ± 0.14) compared with 36°C (1.08 ± 0.19) after 60 minutes (Fig. 6C). The latter observation suggests that the probability of a cAMP molecule to be exported after NE stimulation is higher at 38 as compared with 36°C. Such an elevated export at 38°C may contribute to enhanced cytosolic cAMP accumulation at 36°C. When effects of temperature on total cAMP production by NE were analyzed at 36°C, there was no loss of the cyclic nucleotide (Fig. 6D). In contrast, at 38°C total cAMP production was still significantly reduced by 27% between 20 and 60 minutes (Fig. 6D).

Enhanced NE-Induced cAMP Degradation in mHypoA-2/10 Cells at 38°C. All cAMP accumulation experiments presented so far were performed in the presence of the nonselective PDE inhibitor IBMX, suggesting that cAMP degradation is significantly inhibited. However, because there was still a significant amount of cAMP missing between 20 and 60 minutes at 38°C (Fig. 6D), we wondered whether altered PDE activity might nevertheless contribute to the effects of temperature on NE-induced cAMP accumulation. First, we analyzed a role of the IBMX-independent PDE-8 subtype in this process. Selective inhibition of PDE-8 did not contribute to NE-induced cAMP accumulation (Supplemental Fig. 1), questioning a role for this PDE subtype in the temperature-sensitive signaling of NE. Next, we performed cAMP degradation experiments by incubating exogenous ^{3}H-cAMP for different time periods (10–60 minutes) with homogenates of mHypoA-2/10 cells at 37°C. As shown in Fig. 7A, ^{3}H-cAMP levels decreased over time in the absence but not in the presence of IBMX, and significant ^{3}H-cAMP degradation was observed after 20 minutes onwards. We next stimulated cells with NE for 30 minutes at 37°C without IBMX and then detected ^{3}H-cAMP degradation in the same homogenates at 36 or 38°C after 20 minutes. At both temperatures, significantly less ^{3}H-cAMP was recovered compared with the input (Fig. 7B). Interestingly, the amount of recovered ^{3}H-cAMP was significantly less at 38 compared with 36°C. When ^{3}H-cAMP degradation was calculated as percentage of the corresponding input, degradation increased significantly from 12.7% ± 6.5% at 36°C to 21.2% ± 6.3% at 38°C (Fig. 7C), indicating that PDE activity in NE-stimulated mHypoA-2/10 cells is promoted by physiologic temperature increases, resulting in enhanced NE-induced cytosolic cAMP accumulation at 36°C.

Basal and NE-Induced Thyreoliberin Promoter Activity in mHypoA-2/10 Cells Is Enhanced at 36°C. Herein, we report that transcriptional activity of CREB and STAT is enhanced at 36°C (Fig. 1). The promoter of the thyreoliberin gene exhibits binding sites for CREB and STAT (Harris et al., 2001). Thus, enhanced activity of these transcription

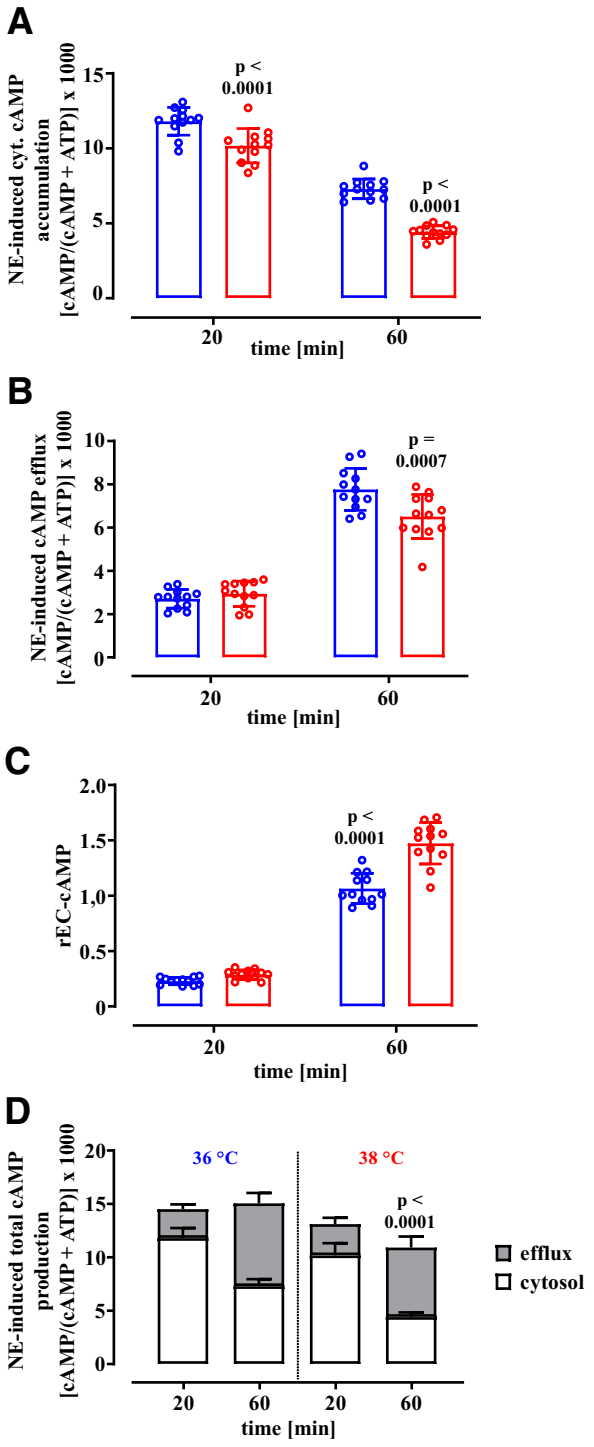

Fig. 6. NE-induced cytosolic cAMP accumulation and efflux are temperature-sensitive. Cytosolic cAMP accumulation (A) and efflux (B) induced by 10 μM NE in the presence of 1 mM IBMX was measured for 20 and 60 minutes at 36 or 38°C. In (C), rEC-cAMP at 20 or 60 minutes were calculated. In (D), data from (A) and (B) were compiled. Blue bars present data obtained at 36°C, red bars data at 38°C. Data of 4 independent experiments performed in triplicates were expressed as the mean ± S.D. Two-way ANOVA followed by Šidák's post hoc test (A–C) or Tukey's post hoc test (D) was used to determine statistical differences.

factors at 36°C could in turn enhance the thyreoliberin promoter. We used mHypoA-2/10 cells expressing a thyreoliberin promoter reporter construct and measured promoter activity at 36 and 38°C over 1 to 4 hours. As shown in Fig. 8A, basal thyreoliberin promoter activity increased at 36 and decreased at 38°C. After 4 hours, promoter activity was significantly different (748 ± 273 RLU at 36°C versus 409 ± 135 RLU at 38°C). NE has also been shown to induce thyreoliberin mRNA expression in the PVN (Grimm and Reichlin, 1973). Thus, we also stimulated thyreoliberin promoter expressing cells for 1 to 4 hours with 10 μM NE at either 36 or 38°C (Fig. 8B). NE enhanced thyreoliberin promoter activity at each time point and temperature. Noteworthy, after 3 hours, x-fold over basal values significantly increased from 0.8 ± 0.3 at 38 to 1.4 ± 0.5 at 36°C.

Temperature Affects Gs- Rather the Gq-Induced CREB Activation. So far, we provide new data indicating that hormone-induced activation of CREB-dependent transcription is increased at 36°C, because of enhanced PDE activity and cAMP efflux at 38°C. In this model, cAMP-dependent but not independent CREB activation should be temperature insensitive. To analyze the correlation between the signaling pathway leading to CREB activation and temperature sensitivity, we compared CREB activity by the adenosine A2B receptor agonist BAY60-6583 and BK. Both ligands induced significant activation of the CREB reporter of 4.5 ± 1.5 and 5.6 ± 2.0 respectively at 37°C (Fig. 9A). As already shown in Fig. 2B, BK induced Ca^{2+} signals in hypothalamic cells, suggesting that BK activates Gq rather than Gs proteins. In contrast, adenosine A2B receptor is more likely to engage with Gs proteins. In line with these assumptions, BAY60-6583 but not BK-induced cAMP accumulation in mHypoA-2/10 cells (Fig. 9B) and BK-mediated cAMP responseelement activity was blunted by the PKC inhibitors BIM-X and Gö6983 (Fig. 9C). Interestingly, when effects of temperature were analyzed on BAY60-6583- and BK-induced CREB activation, enhanced activity was observed at 36°C for BAY60-6583 but not for BK (Fig. 9D). Hence, we put forward a model in which temperature affects specifically Gs- and not Gq-promoted CREB activation, which is in line with the observed effects of temperature on PDE activity and cAMP efflux.

36°C Enhanced NE- or Sal-Induced cAMP Accumulation in Various Cell Lines. Our data obtained in mHypoA-2/10 cells raise the question of whether temperature effects on β_2-AR–induced cAMP signaling is restricted to these cells or a rather common phenomenon. Thus, we aimed at analyzing the temperature sensitivity of NE- and Sal-induced cAMP accumulation in a second hypothalamic cell line (mHypoA-2/12 cells), in lung cells (H1299 cells), in keratinocytes (HaCaT cells), and in primary HBSMC. First, we determined NE-induced cAMP accumulation at 37°C, to compare efficacy of NE in these cells (Fig. 10A). We found a rank order of efficacy of HaCaT ≫ H1299 > HBMSC = mHypoA-2/10 = mHypoA-2/12. When cAMP accumulation obtained at 38°C was set to 100%, efficacy of NE at 36°C significantly increased to 123% ± 14% in mHypoA-2/12 cells, to 114% ± 15% in H1299 cells, and to 115% ± 15% in HBSMC. Efficacy of Sal was significantly enhanced to 120% ± 8% in mHypoA-2/12 cells and to 122% ± 22% in H1299 cells (Fig. 10, B–E).

Discussion

Although it is established that CBT fluctuates ±1°C, most of our knowledge about cellular signaling induced by hormones is based on data obtained with cells analyzed at the

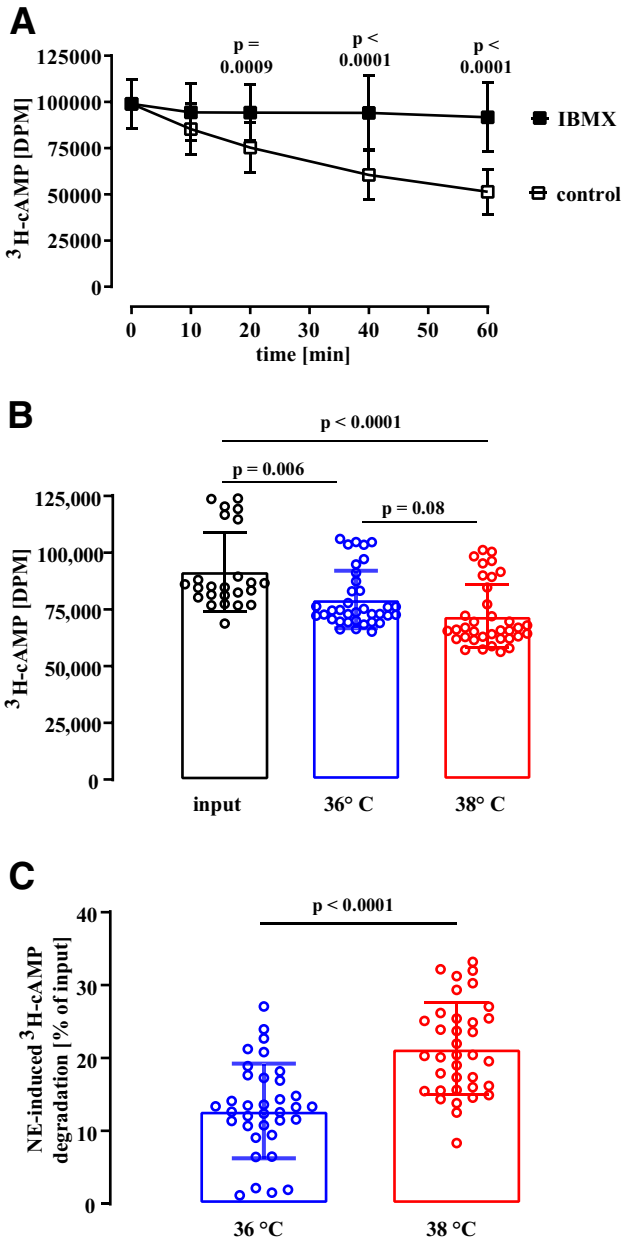

Fig. 7. NE-induced ^{3}H-cAMP degradation is enhanced at 38°C. In (A), ^{3}H-cAMP degradation in homogenates from unstimulated cells was measured for 10, 20, 40, or 60 minutes with or without 1 mM IBMX at 37°C. As a control (input), the same amount of ^{3}H-cAMP was incubated without homogenates and also purified. No statistical differences between homogenates with IBMX and the input control were observed (data not shown). In (B and C), ^{3}H-cAMP degradation in homogenates of cells treated with 10 μM NE for 30 minutes at 37°C without IBMX was measured for 20 minutes at 36 or 38°C. Blue bars present data obtained at 36°C, red bars data at 38°C. In (B), raw data are shown as ^{3}H-cAMP in decays per minute. In (C), ^{3}H-cAMP degradation was calculated as percentage of the corresponding input control. 7 independent experiments performed in triplicates were expressed as the mean ± S.D. Two-way ANOVA followed by Šidák's post hoc test was used in (B) and two-tailed *t* test in (C) to determine statistical differences.

average CBT of 37°C. Cellular signaling is the result of consecutive interactions of small molecules with proteins, protein-protein interactions, and enzymatic reactions. Each of these steps is potentially temperature-dependent, and even small effects on each single level could sum up to significant effects at the end of the signaling pathway.

Herein, we used a murine hypothalamic cell line (mHypoA-2/10 cells) as an in vitro model system and cell incubators with a temperature accuracy that allowed challenging cells with temperature changes in the physiologic range of ±1°C with the average CBT as the baseline. A span in temperature changes of ±1°C seems reasonable, because it is well in the range of the CBT changes observed in mice and humans, and an established protocol to mimic changes in CBT in vitro (Refinetti and Menaker, 1992; Buhr et al., 2010; Breit et al., 2018). We have chosen mHypoA-2/10 cells because they have previously been shown to be temperature-sensitive when the promoter of the clock gene BMAL1 was used as a read-out (Breit et al., 2018). Secondly, these cells show several characteristics of PVN neurons, which have been reported to express high levels of β-AR (Little et al., 1992; Breit et al., 2015). Here, we report firstly, based on mRNA analysis and the use of subtype specific agonists and antagonists, that β_2- and β_3-AR subtypes are endogenously expressed in mHypoA-2/10 cells at levels that allow to study ligand binding, cAMP signaling, and gene reporter activity induced by catecholamines in their natural, cellular environment. Hence, we exposed these cells to temperatures that mimic changes in CBT and analyzed the pharmacodynamics of NE.

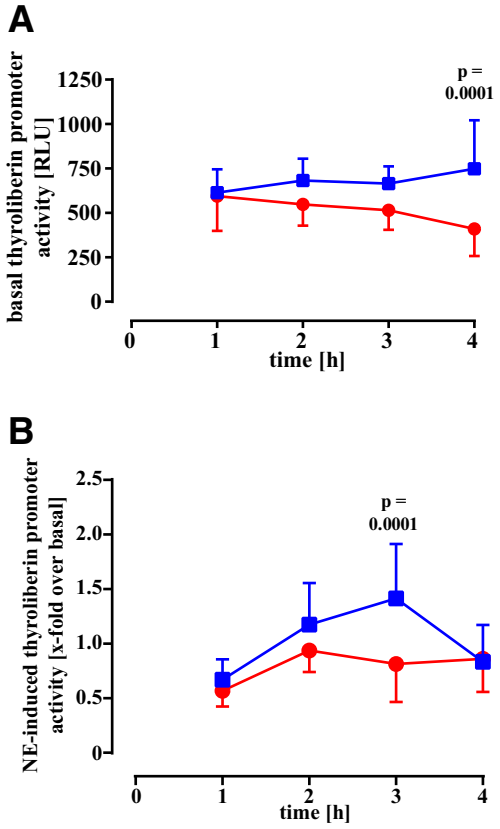

Fig. 8. Basal and NE-induced thyreoliberin promoter activity is increased at 36°C. Thyreoliberin promoter activity was monitored using mHypoA-2/10 cells stably expressing a luciferase promoter construct encoding the rat thyreoliberin promoter. Basal and NE (10 μM)-induced promoter activity was measured for 1, 2, 3, and 4 hours at 36°C (blue bars) or 38°C (red bars). In (A), basal reporter activity is given in RLU. In (B), x-fold over basal values of NE-stimulated cells are provided. Data of 4 independent experiments performed in triplicates were expressed as the mean ± S.D. Two-way ANOVA followed by Šidák's post hoc test was used to determine statistical differences.

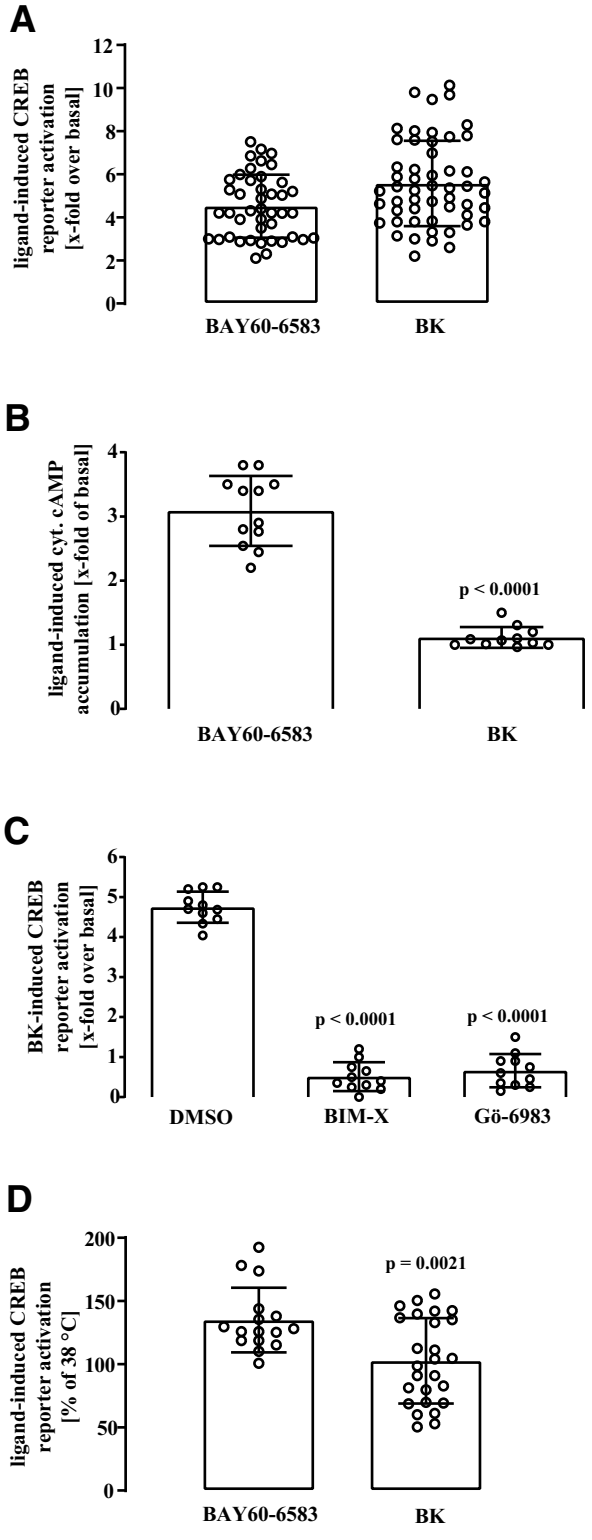

Fig. 9. BAY60-6583 but not BK-induced CREB activation is enhanced at 36°C. In (A, B, and D), data using cells stably expressing the CREB-dependent luciferase reporter are shown. In (C), ligand-induced cytosolic cAMP accumulation is given as x-fold of basal after stimulation of cells with BAY60-6583 or BK (both 1 μM) at 37°C for 30 minutes. Data of 3 independent experiments performed in triplicates are compiled as the mean ± SD and two-tailed *t* test performed to determine statistical differences. In (A), CREB reporter–expressing mHypoA-2/10 cells were stimulated for 4 hours at 37°C with BAY60-6583 or BK (both 1 μM). Data of 3 independent experiments performed in triplicates are compiled as the mean ± SD and two-tailed *t* test performed to determine statistical differences. In (C), cells were preincubated with the PKC inhibitors BIM-X or Gö6983 (both 10 μM) and the stimulated with BK (1 μM) for 4 hours at 37°C. Data of 3 independent experiments performed in triplicates are compiled as the mean ± SD, and one-way ANOVA followed by Šidák's post hoc test used to determine statistical differences. In (D), cells were either incubated for 4 hours at 36 or 38°C and then for additional 4 hours stimulated with BAY60-6583 or BK (both 1 μM). Bars in red indicate data obtained at 38°C, bars in blue at 36°C. Data obtained at 38°C were set to 100%. Two-tailed *t* test was performed to determine statistical differences.

We found that affinity and potency of NE is temperature-independent, whereas efficacy to induce cytosolic cAMP accumulation was enhanced at 36°C compared with 37°C, and even more pronounced when compared with 38°C. Binding assays were performed when ligand binding reached equilibrium. Thus, at this point, we cannot exclude that the kinetics of agonist binding to the β_2-AR (e.g., association or dissociation constants) are temperature-dependent. Furthermore, based on the low affinity of the β_3-AR to the radiolabeled tracer used, we cannot comment on the temperature sensitivity of the agonist binding to this receptor subtype. We also cannot exclude a role for G protein or AC activity in the temperature sensitivity of NE-induced cAMP accumulation. The independence of the Gpp(NH)p-sensitive fraction to temperature observed in the displacement experiment with Sal (Fig. 3; Table 1) suggests that agonist-induced interactions between β_2-AR and G proteins might be temperature-independent. Similarly, temperature sensitivity of NE-induced cAMP accumulation was not affected by the $G_{i/o}$ inhibitor *pertussis toxin* (data not shown). However, further studies with direct measurements of G protein and AC activity induced by NE are required to define finally the role for these processes in the temperature dependence of NE-induced cAMP accumulation.

Cytosolic cAMP accumulation is the result of cAMP production by AC and degradation by PDE. Because we performed the cAMP accumulation assay in the presence of IBMX, a role for PDE in the temperature dependence of NE-induced cAMP accumulation seemed unlikely. However, based on the data shown in Fig. 6D, it appeared that PDE inhibition was not complete. Thus, we validated sensitivity of PDE toward temperature by performing PDE activity assays. Here, we found that ^{3}H-cAMP degradation in the homogenates of cells stimulated with NE is significantly higher at 38 compared with 36°C. Noteworthy, in these experiments, NE stimulation was performed at 37°C, and the same pool of homogenates was used to detect degradation at 36 and 38°C, excluding potential effects of temperature on the processes leading to cAMP production (e.g., G protein or AC activity). Hence, we provide significant new data indicating that cAMP degradation in NE-challenged hypothalamic cells is increased at 38 compared with 36°C. This model raises the question of the identity of the temperature-sensitive PDE subtype. mRNA sequencing data revealed expression of 8 different PDE subtypes (PDE1a, PDE1b, PDE3b, PDE4a, PDE4b, PDE7a, PDE8a, PDE12) in mHypoA-2/10 cells with a reads per kilobase of transcript per million reads mapped ≥2.0. Hence, any of these PDE subtypes could potentially be temperature-sensitive. Further studies using specific siRNA and small molecule inhibitors are required to determine the PDE subtype(s) responsible for the temperature sensitivity of NE-induced cAMP signaling. Of note, recent studies advanced

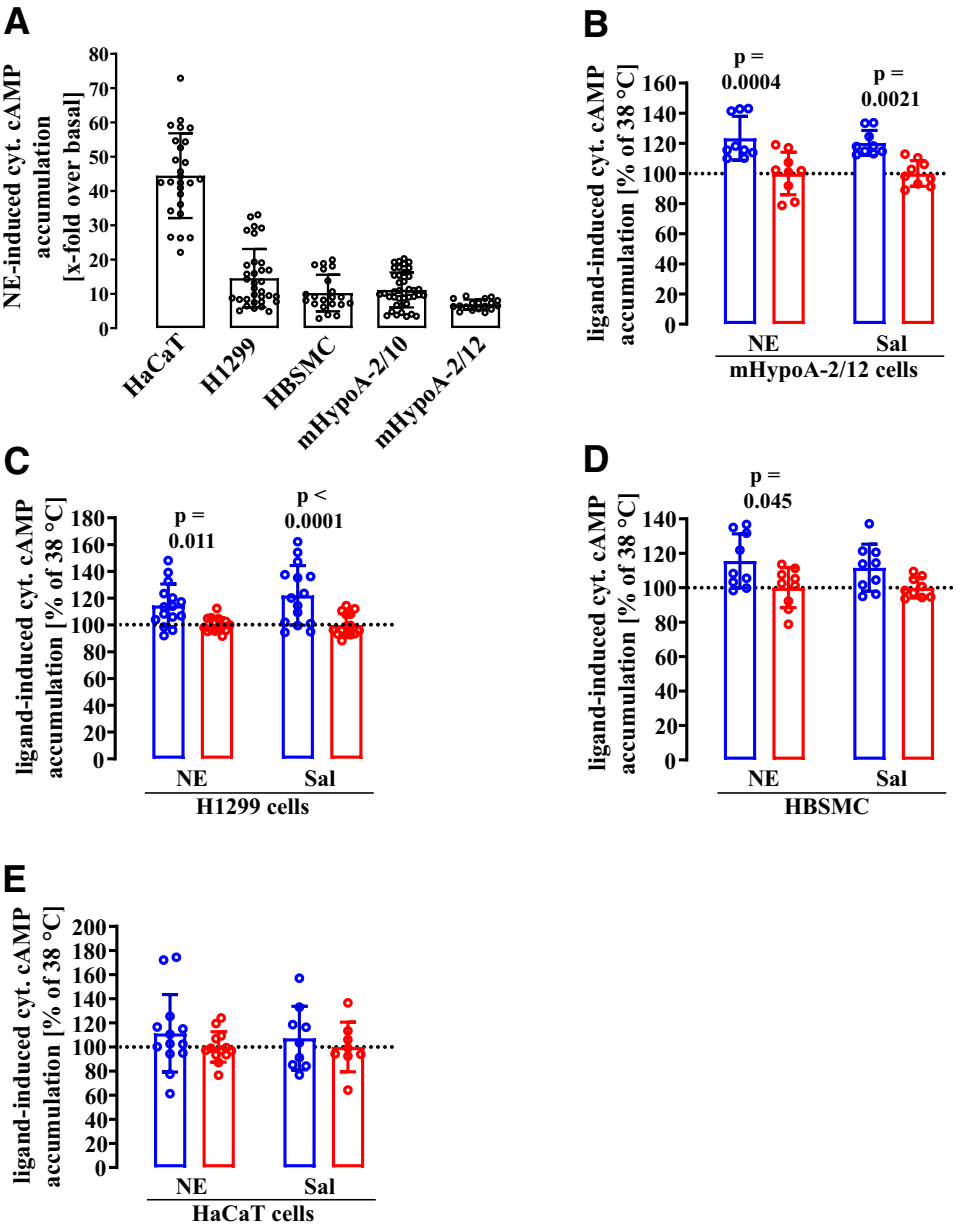

Fig. 10. NE- or Sal-induced cAMP accumulation is enhanced at 36°C in various cell lines. cAMP accumulation was measured after stimulation of cells with NE (10 μM) at 37°C (A) or at 36 and 38°C with NE (10 μM) or Sal (100 nM) in (B–E). In (A), data of 5 independent experiments performed in quadruplicates are compiled as the mean ± SD. In (B), mHypoA-2/12 cells, in (C), H1299 cells, in (D), primary HBSMCs, and in (E), data of HaCaT cells are shown. Bars in red indicate data obtained at 38°C, bars in blue at 36°C. Data obtained at 38°C were set to 100%. Two-way ANOVA followed by Šidak's post hoc test was used to determine statistical differences.

our understanding of cAMP signaling by revealing that distinct intracellular cAMP pools have specific signaling properties (Zaccolo et al., 2021). Different intracellular expression patterns of distinct PDE subtypes contribute to these cytosolic cAMP pools. Thus, specific effects of temperature on certain PDE subtypes in particular areas of the cell could lead to exclusive temperature dependence of cAMP signaling within these areas. The use of cAMP-dependent FRET probes and confocal microscopes could help to reveal these specific effects of temperature on particular cAMP pools within the cell (Adams et al., 1991).

We postulate that other processes besides PDE activity are also responsible for the temperature sensitivity of NE-induced cAMP signaling. Similar to other cell types, we observed NE-induced efflux from mHypoA-2/10 cells (Godinho et al., 2015). Interestingly, NE-induced net cAMP efflux was higher at 36 compared with 38°C after 60 minutes, but not after 20 minutes (Fig. 6B). However, after NE stimulation, the rEC-cAMP was higher at 38°C. This increased rEC-cAMP value may reflect an enhanced efflux at 38°C, a factor that could also account for enhanced cytosolic cAMP concentrations at 36°C. We developed a model in Fig. 10 which suggests that a combination of enhanced PDE and ABCC activity at 38°C determines NE-induced signaling, such that the cytosolic cAMP concentration is increased at 36°C, but the rEC-cAMP at 38°C. However, further studies using siRNA against distinct ABCC subtypes are required to validate finally their contribution to the enhanced NE-induced cytosolic cAMP accumulation and their interplay with PDEs. At this point, the physiologic role of cAMP efflux from hypothalamic cells is unknown. In other tissues, extracellular cAMP has been shown to be converted into adenosine and thus to activate members of the adenosine receptor family (Godinho et al., 2015). Assuming a similar role of extracellular cAMP in the interstitium of hypothalamic neurons, temperature may appear as a significant modulator of this

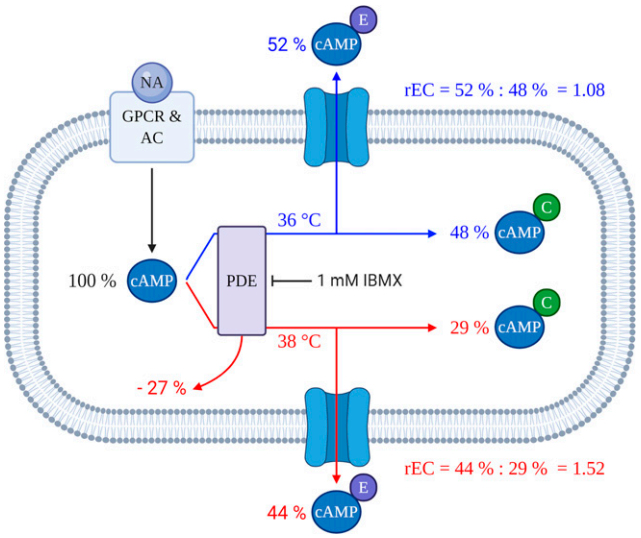

Fig. 11. Increased temperature decreases NE-induced cytosolic cAMP accumulation by enhancing PDE activity and cAMP efflux. A model based on the data shown in Fig. 6 is depicted. Assuming that NE-induced cAMP production in mHypoA-2/10 cells is temperature-insensitive, we set the amount of original produced cAMP to 100%. At 36°C (blue path), no cAMP is degraded in the presence of the PDE inhibitor IBMX (1 mM). Thus, the entire cAMP pool is available for cAMP transporters. 52% of this pool is exported and 48% remains in the cell, resulting in a rEC-cAMP of 1.08. At 38°C (red path), around 27% of the produced cAMP is degraded, 44% exported and 29% remains in the cytosol. Thus, resulting in a rEC-cAMP of 1.52.

process, which might be of particular interest when considering the importance of the adenosine-1-receptor subtype in the PVN (Wu et al., 2017).

Here, we provide new evidence that physiologic temperature alterations modulate basal CREB- or STAT-dependent reporter activity in hypothalamic cells. Thyreoliberin mRNA levels peak at the end of the resting cool phase (Covarrubias et al., 1988). However, it is not fully understood which signal pathways control circadian thyreoliberin expression on the level of the promoter. The thyreoliberin promoter contains cAMP and STAT sites, and thyreoliberin mRNA levels in the hypothalamus peak at the end of the resting cool phase (Covarrubias et al., 1988; Harris et al., 2001). Thus, assuming that temperature-sensitive CREB and/or STAT activity translates into altered thyreoliberin promoter activity, our data provide an interesting new molecular basis for circadian expression of thyreoliberin. This notion is supported by our data, showing that basal thyreoliberin promoter activity is indeed enhanced at 36°C. However, it needs further investigations to dissect whether temperature sensitivity of either CREB or STAT is responsible for the enhanced thyreoliberin promoter activity. So far, it has been reported that the NE system is less active in the resting state because AR expression and NE serum levels are reduced at cooler temperature (Kafka et al., 1981; Pangerl et al., 1990; Leach and Suzuki, 2020). Our data, indicating that efficacy of NE is increased at 36°C, suggest that, despite decreased receptor and hormone levels in the resting phase, the impact of NE on cAMP signaling might even be increased. However, it requires animal experiments to analyze 1) whether NE-induced cAMP accumulation is also enhanced in the resting state in vivo and 2) whether this increase compensates for the reduced hormone and receptor levels. Here we provide first data, showing that, in the presence of NE thyreoliberin, promoter activity is significantly higher at 36 compared with 38°C. Thus, enhanced efficacy of NE in the resting state could contribute to increased thyreoliberin promoter activity in this state.

We present first evidence indicating that physiologically relevant temperature fluctuations affect catecholamine-induced signaling in murine, hypothalamic mHypoA-2/10 cells. These data raise the question of how specific these effects are. We found several indications that temperature changes in the range of ±1°C do not affect overall signaling. Temperature affected 1) basal STAT and CREB but not FOXO activity, 2) NE-, FSK-, and BAY60-658- but not BK-induced CREB or IFNγ-promoted STAT activation, and 3) NE-induced cAMP accumulation but not ligand binding. Hence, we suggest that temperature specifically affects Gs- and not Gq-promoted CREB activation, due to the observed effects of temperature on PDE activity and cAMP efflux. In this context, it might be worth mentioning that temperature enhanced efficacy of Sal by 62% ± 33% and of NE by 45% ± 27% (P value = 0.04, t test), suggesting that temperature might even affect distinct β_2-AR agonists differently. This may be related to the selectivity of Sal to the β_2-AR in contrast to the unselective interaction of NE with β_2- and β_3-AR, in particular, when considering that both receptors are expressed in mHypoA-2/10 cells. However, it requires further studies to dissect the temperature sensitivity of different β-AR ligand receptor pairs.

Our data obtained in one hypothalamic cell line raise also the question whether this effect is restricted to these cells or an overall phenomenon. We further tested efficacy of NE and Sal to induce cAMP accumulation in a second hypothalamic cell line, in lung cells, in keratinocytes, and primary bronchial smooth muscle cells. With the exception of the keratinocytes, all cells exhibited significantly increased efficacy of NE at 36°C and hypothalamic and lung cells also for Sal. Although these effects were less pronounced, physiologic temperature alterations may function as a general regulator of catecholamine-induced cAMP signaling.

Authorship Contributions

Participated in research design: Faro, Boekhoff, Gudermann, Breit.

Conducted experiments: Faro, Breit.

Performed data analysis: Faro, Breit.

Wrote or contributed to the writing of the manuscript: Faro, Boekhoff, Gudermann, Breit.

References

Adams SR, Harootunian AT, Buechler YJ, Taylor SS, and Tsien RY (1991) Fluorescence ratio imaging of cyclic AMP in single cells. *Nature* **349**:694–697.

Belsham DD, Fick LJ, Dalvi PS, Centeno ML, Chalmers JA, Lee PK, Wang Y, Drucker DJ, and Koletar MM (2009) Ciliary neurotrophic factor recruitment of

glucagon-like peptide-1 mediates neurogenesis, allowing immortalization of adult murine hypothalamic neurons. *FASEB J* **23**:4256–4265.
Breit A, Besik V, Solinski HJ, Muehlich S, Glas E, Yarwood SJ, and Gudermann T (2015) Serine-727 phosphorylation activates hypothalamic STAT-3 independently from tyrosine-705 phosphorylation. *Mol Endocrinol* **29**:445–459.
Breit A, Miek L, Schredelseker J, Geibel M, Merrow M, and Gudermann T (2018) Insulin-like growth factor-1 acts as a zeitgeber on hypothalamic circadian clock gene expression via glycogen synthase kinase-3β signaling. *J Biol Chem* **293**:17278–17290.
Brodde OE, Kuhlhoff F, Arroyo J, and Prywarra A (1983) No evidence for temperature-dependent changes in the pharmacological specificity of beta 1- and beta 2-adrenoceptors in rabbit lung membranes. *Naunyn Schmiedebergs Arch Pharmacol* **322**:20–28.
Brunet A, Bonni A, Zigmond MJ, Lin MZ, Juo P, Hu LS, Anderson MJ, Arden KC, Blenis J, and Greenberg ME (1999) Akt promotes cell survival by phosphorylating and inhibiting a Forkhead transcription factor. *Cell* **96**:857–868.
Buhr ED, Yoo SH, and Takahashi JS (2010) Temperature as a universal resetting cue for mammalian circadian oscillators. *Science* **330**:379–385.
Chuang DM, Dillon-Carter O, Spain JW, Laskowski MB, Roth BL, and Coscia CJ (1986) Detection and characterization of beta-adrenergic receptors and adenylate cyclase in coated vesicles isolated from bovine brain. *J Neurosci* **6**:2578–2584.
Covarrubias L, Uribe RM, Méndez M, Charli JL, and Joseph-Bravo P (1988) Neuronal TRH synthesis: developmental and circadian TRH mRNA levels. *Biochem Biophys Res Commun* **151**:615–622.
De Blasi A (1990) Beta-adrenergic receptors: structure, function and regulation. *Drugs Exp Clin Res* **16**:107–112.
Godinho RO, Duarte T, and Pacini ES (2015) New perspectives in signaling mediated by receptors coupled to stimulatory G protein: the emerging significance of cAMP eux and extracellular cAMP-adenosine pathway. *Front Pharmacol* **6**:58.
Grimm Y and Reichlin S (1973) Thyrotropin releasing hormone (TRH): neurotransmitter regulation of secretion by mouse hypothalamic tissue in vitro. *Endocrinology* **93**:626–631.
Harris M, Aschkenasi C, Elias CF, Chandrankunnel A, Nillni EA, Bjøorbaek C, Elmquist JK, Flier JS, and Hollenberg AN (2001) Transcriptional regulation of the thyrotropin-releasing hormone gene by leptin and melanocortin signaling. *J Clin Invest* **107**:111–120.
Kafka MS, Wirz-Justice A, and Naber D (1981) Circadian and seasonal rhythms in alpha- and beta-adrenergic receptors in the rat brain. *Brain Res* **207**:409–419.
Keirns JJ, Kreiner PW, and Bitensky MW (1973) An abrupt temperature-dependent change in the energy of activation of hormone-stimulated hepatic adenylyl cyclase. *J Supramol Struct* **1**:368–379.
Kouidhi S, Seugnet I, Decherf S, Guissouma H, Elgaaied AB, Demeneix B, and Clerget-Froidevaux MS (2010) Peroxisome proliferator-activated receptor-gamma (PPARgamma) modulates hypothalamic Trh regulation in vivo. *Mol Cell Endocrinol* **317**:44–52.
Kreiner PW, Keirns JJ, and Bitensky MW (1973) A temperature-sensitive change in the energy of activation of hormone-stimulated hepatic adenylyl cyclase. *Proc Natl Acad Sci USA* **70**:1785–1789.
Leach S and Suzuki K (2020) Adrenergic signaling in circadian control of immunity. *Front Immunol* **11**:1235.
Lefkowitz RJ, Stadel JM, Cerione RA, Strulovici B, and Caron MG (1984) Structure and function of beta-adrenergic receptors: regulation at the molecular level. *Adv Cyclic Nucleotide Protein Phosphorylation Res* **17**:19–28.
Little KY, Duncan GE, Breese GR, and Stumpf WE (1992) Beta-adrenergic receptor binding in human and rat hypothalamus. *Biol Psychiatry* **32**:512–522.
Lotti VJ, Kling P, and Cerino D (1982) High and low (Gpp(NH)p-sensitive) affinity sites for beta 2-adrenergic blockers as antagonists of isoproterenol in the field-stimulated rat vas deferens. *Eur J Pharmacol* **84**:161–167.
Low FG, Shabir K, Brown JE, Bill RM, and Rothnie AJ (2020) Roles of ABCC1 and ABCC4 in proliferation and migration of breast cancer cell lines. *Int J Mol Sci* **21**:E7664.
Miyamoto S, Hori M, Izumi M, Ozaki H, and Karaki H (2001) Species- and temperature-dependency of the decrease in myofilament Ca2+ sensitivity induced by beta-adrenergic stimulation. *Jpn J Pharmacol* **85**:75–83.
Niclauss N, Michel-Reher MB, Alewijnse AE, and Michel MC (2006) Comparison of three radioligands for the labelling of human beta-adrenoceptor subtypes. *Naunyn Schmiedebergs Arch Pharmacol* **374**:99–105.
Pangerl B, Pangerl A, and Reiter RJ (1990) Circadian variations of adrenergic receptors in the mammalian pineal gland: a review. *J Neural Transm (Vienna)* **81**:17–29.
Refinetti R and Menaker M (1992) The circadian rhythm of body temperature. *Physiol Behav* **51**:613–637.
Reinhardt D, Butzheinen R, Brodde OE, and Schümann HJ (1978) The role of cyclic AMP in temperature-dependent changes of contractile force and sensitivity ot isoprenaline and papaverine in guinea-pig atria. *Eur J Pharmacol* **48**:107–116.
Reynolds CH and Holloway MK (2011) Thermodynamics of ligand binding and efficiency. *ACS Med Chem Lett* **2**:433–437.
Samama P, Cotecchia S, Costa T, and Lefkowitz RJ (1993) A mutation-induced activated state of the beta 2-adrenergic receptor. Extending the ternary complex model. *J Biol Chem* **268**:4625–4636.
Strosberg AD (1993) Structure, function, and regulation of adrenergic receptors. *Protein Sci* **2**:1198–1209.
Tank AW and Lee Wong D (2015) Peripheral and central effects of circulating catecholamines. *Compr Physiol* **5**:1–15.
Wada H, Osborne Jr JC, and Manganiello VC (1987) Effects of temperature on allosteric and catalytic properties of the cGMP-stimulated cyclic nucleotide phosphodiesterase from calf liver. *J Biol Chem* **262**:5139–5144.
Walsh KB, Begenisich TB, and Kass RS (1989) Beta-adrenergic modulation of cardiac ion channels. Differential temperature sensitivity of potassium and calcium currents. *J Gen Physiol* **93**:841–854.
Wu L, Meng J, Shen Q, Zhang Y, Pan S, Chen Z, Zhu LQ, Lu Y, Huang Y, and Zhang G (2017) Caffeine inhibits hypothalamic A_1R to excite oxytocin neuron and ameliorate dietary obesity in mice. *Nat Commun* **8**:15904.
Ye L, Wu J, Cohen P, Kazak L, Khandekar MJ, Jedrychowski MP, Zeng X, Gygi SP, and Spiegelman BM (2013) Fat cells directly sense temperature to activate thermogenesis. *Proc Natl Acad Sci USA* **110**:12480–12485.
Zaccolo M, Zerio A, and Lobo MJ (2021) Subcellular organization of the cAMP signaling pathway. *Pharmacol Rev* **73**:278–309.

Address correspondence to: Dr. Andreas Breit, Goethestrasse 33, Walther-Straub-Institut für Pharmakologie und Toxikologie, Ludwig-Maximilians-Universität München, 80336 München, Germany. E-mail: andreas.breit@lrz.uni-muenchen.de